HOKKAIDO UNIVERSITY

Title	Adsorption and co-precipitation behavior of arsenate, chromate, selenate and boric acid with synthetic allophane-like materials
Author(s)	Opiso, Einstine; Sato, Tsutomu; Yoneda, Tetsuro
Citation	Journal of Hazardous Materials, 170(1), 79-86 https://doi.org/10.1016/j.jhazmat.2009.05.001
Issue Date	2009-10-15
Doc URL	https://hdl.handle.net/2115/39258
Type	journal article
File Information	JHM170-1_p79-86.pdf

Hokkaido University Collection of Scholarly and Academic Papers : HUSCAP

Adsorption and co-precipitation behavior of arsenate, chromate, selenate and boric acid with synthetic allophane-like materials

*Einstine OPISO[1], Tsutomu SATO[1] and Tetsuro YONEDA[1]

Laboratory of Environmental Geology

Division of Solid Waste, Resources and Geoenvironmental Engineering

Graduate School of Engineering, Hokkaido University

Kita 13 Nishi 8, Kita-ku, Sapporo 060-8628 Japan

Corresponding Author:

Einstine M. Opiso

Laboratory of Environmental Geology, Graduate School of Engineering

Hokkaido University, Kita 13 Nishi 8 Kita-ku, Sapporo 060-8628 Japan

Tel.: +81-11-706-6839,

Fax: +81-11-706-6839

Email: einstine@eng.hokudai.ac.jp

Abstract

Pollution caused by boric acid and toxic anions such as As(V), Cr(VI) and Se(VI) is hazardous to human health and environment. The sorption characteristics of these environmentally significant ionic species on allophane-like nanoparticles was investigated in order to determine whether allophane can reduce their mobility in the subsurface environment at circum-neutral pH condition. Solutions containing 100 or 150 mmol of $AlCl_3$. $6H_2O$ were mixed to 100 mmol of Na_4SiO_4 and the pH were adjusted to 6.4±0.3. The mineral suspensions were shaken for 1 hr and incubated at 80^oC for 5 days. Appropriate amounts of As, B, Cr and Se solutions were added separately during and after allophane precipitation. The results showed that As(V) and boric acid can be irreversibly fixed during co-precipitation in addition to surface adsorption. However, Cr(VI) and Se(VI) retention during and after allophane precipitation is mainly controlled by surface adsorption. The structurally fixed As(V) and boric acid were more resistant to release than those bound on the surface. The sorption characteristics of oxyanions and boric acid was also influenced by the final Si/Al molar ratio of allophane in which Al-rich allophane tend to have higher uptake capacity. The overall results of this study have demostrated the role of allophane-like

nanoparticles and the effect of its Si/Al ratio on As, B, Cr and Se transport processes in the subsurface environment.

Keywords: allophane, adsorption, co-precipitation, oxyanions, boric acid

1. Introduction

Contamination of environmental media caused by toxic elements such as arsenic, boron, chromium and selenium is receiving increasing attention due to their potentially hazardous risk to public health and the environment. These toxic elements are introduced into the environment from a variety of natural (e.g. geothermal processes and mineral weathering) and anthropogenic (e.g. mining industries and agriculture) sources and highly mobile at pH condition typical of most hydrogeological environments. Their high mobility at near neutral pH condition is attributed to their anionic character (except for boron with neutral charge), which results to their low adsorption onto negatively charged soil surfaces. Moreover, the mobility and distribution of ionic species in natural systems are largely controlled by adsorption and incorporation at mineral phases [1]. Among the mineral phases that can control the mobility of anionic species in circum-neutral to alkaline environments include hydroxylapatite for arsenate [2],

hydrotalcite for boron [3], calcite for chromate [4] and ettringite for selenate [5].

Allophane naturally exists as an aluminosilicate hydrate mineral with no fixed chemical composition in that its Si/Al molar ratio may vary from 0.5 to 1.0. The unit particle of allophane is a hollow spherule with an outer diameter of 3.5- 5.0 nm and a wall thickness of 0.7-1.0 nm [6, 7]. Allophane is fundamentally composed of an outer layer of gibbsite-like sheet with SiO_4 tetrahedral attached to its interior and having defects or pores in the wall structure with diameters of around 0.3 nm [8]. Figure 1 shows the structural model of allophane.

The substantial retention capacity of allophane for anions particularly for phosphate is ascribed to its small particle size, high surface area (800 m^2/g), and the presence at the surface of aluminol groups and defect sites [9]. Hence, understanding the interaction of allophane with toxic anions has environmental implications since this type of mineral is commonly present in volcanic ash soils, pumice deposits and stream sediments which are exposed to various anthropogenic sources of environmental contamination. Recent studies also revealed that the weathering of coal fly ash, which usually contain toxic oxyanions, generate large amount of non-crystalline aluminosilicate clay minerals such as allophane and imogolite which can possibly sequester these trace elements [10].

A considerable amount of research, which investigated anion adsorption by

allophane, has reported and concluded that the anions such as As(V) are specifically adsorbed and form inner-sphere complexes by reacting with the aluminol functional groups present in the allophane surface. X-ray Absorption Spectroscopic (XAS) analysis on arsenate adsorption onto allophane-like materials suggests that bidentate binuclear reaction occurred on aluminum octahedral structures [11]. Studies on sulfate, molybdate and borate adsorption by natural allophane samples also showed similar result in which the uptake mechanism is via ligand exchange reaction and allophane with lower Si/Al molar ratio tends to retain more anions than allophane with Si/Al molar ratio close to 1.0 [12, 13, 14]. However, retention by adsorption on the mineral surface with variable charge characteristics would be unstable in the long run as changes in the surrounding environment would release back the adsorbed anions. Therefore, significant immobilization of toxic anions can be achieved only through solid solution formation.

In this context, this study investigated the uptake of As(V), Cr(VI), Se(VI) and boric acid during and after allophane precipitation at near neutral pH condition. The co-precipitation behavior of these toxic anions (except for B) with allophane at circum-neutral pH condition has not been elucidated yet. The present aim of this paper is to examine and compare the co-precipitation and adsorption characteristics of As(V), Cr(VI), Se(VI) and boric acid onto allophane. The possible desorption of co-precipitated

As(V), Cr(VI), Se(VI) and boric acid with allophane by phosphate was also carried out in order to evaluate if incorporation of these toxic anions (except for B) in the allophane structure could be a potential mechanism for controlling their mobility in the geological environment enriched with aluminosilicate minerals. Furthermore, the effect of the Si/Al molar ratio of allophane on the sorption and desorption characteristics of As(V), Cr(VI), Se(VI) and boric acid was also investigated in order to provide vital information for understanding the link between the structure and reactivity of allophane.

2. Materials and methods

2.1 Allophane synthesis

Allophane precipitates were made by modifying the method of Ohashi [15]. Batch experiments were conducted by mixing 100 mL of 100 mM Na_4SiO_4 solution and 100 mL of 100 or 150 mM $AlCl_3.6H_2O$ solution at ambient temperature to obtain an initial Si/Al molar ratio of 1.0 and 0.67, respectively. The suspension pH was adjusted to near neutral (pH 6.4±0.3) by adding 1M NaOH solution. The mineral suspensions were transferred to 250 mL polypropylene bottles and were shaken for 1 hr using a reciprocating shaker. The suspensions were incubated for 5 days at 80 ^{o}C. The

precipitates were collected by centrifugation at 15000 rpm for 30 minutes and washed with deionized water to remove the entrained salt. The morphology of the precipitates was examined by transmission electron microscope and revealed the clustered spherical structure similar to natural and synthetic allophane materials as shown in Figure 2.

2.2 Sorption experiments

The sorption of As(V), Cr(VI), Se(VI) and boric acid was conducted during and after allophane precipitation at circum-neutral pH condition (pH = 6.4±0.3). Appropriate amounts of $Na_2HAsO_4.7H_2O$, $B(OH)_3$, $Na_2CrO_4.4H_2O$ and Na_2SeO_4 solutions were added, respectively to obtain a final As, B, Cr and Se concentration of 10 mg/L (ppm). For adsorption experiments, As(V), Cr(VI), Se(VI) and boric acid solution were added after allophane synthesis and the suspensions were shaken for one day at room temperature. The precipitates were collected by centrifugation at 15000 rpm for 30 minutes. The supernatant was collected and analysed for remaining As, B, Cr and Se concentrations by using inductively coupled plasma-atomic emission spectroscopy (ICP-AES) (ICPE-9000 Shimadsu, Japan). The precipitates were then resuspended in 150mL deionised water and were shaken for 2 hrs prior to centrifugation at 3000 rpm for 40 minutes. This washing process was repeated several times until the conductivity

of the mineral suspension was less than 0.08 dS/m. The precipitates were then kept in suspension prior to any analysis.

2.3 Characterization of allophane precipitates

The precipitates were collected by centrifugation from aliquot samples of washed mineral suspension. The precipitates were freeze dried and were then analysed for characterization.

2.3.1 X-ray diffraction (XRD) analysis

The mineral precipitates were examined using X-ray diffraction on randomly oriented powder mounts. Powder X-ray diffraction measurement was carried out using RINT-2100V/PCdiffractometer (Rigaku, Japan) with Ni-filtered Cu-Kα radiation at 30 kV and 20 mA. The samples were scanned from 5 to 70^0 2θ using a step size of 0.05^0 2θand scanning for 2s for each step.

2.3.2 FTIR spectroscopy of allophane samples

The spectra of allophane samples were obtained by using attenuated total reflectance (ATR)-Fourier Transform Infrared (FTIR) spectroscopy (JASCO FT/IR 6200, UK).

Appropriate amount of allophane samples were placed in the sample holder and then measured at a resolution of 4 cm^{-1} in the 400 – 4000 cm^{-1} range and scanned 300 times.

2.3.3 Surface charge determination

The zeta potential (ZP) of the allophane samples was measured using Zetasizer Nano ZS90 (MALVERN Instruments, UK). Appropriate amount of freeze dried samples were resuspended in 10 mL deionised water to obtain a final mineral concentraion of 100 mg/L. The auto-titration was initiated from pH 3 to 10 and the pH was adjusted by using dilute concentration of HNO_3 and NaOH solutions. The zeta potentials were calculated using the Smoluchowski equation. The Point of Zero Charge (PZC) was determined from the corresponding zero value of ZP.

2.4 Chemical analysis

The compositions of the allophane samples were determined by dissolving the freeze dried samples in ammoniumoxalate-oxalic acid (TAO) solution. Approximately 20 mg of each mineral samples was placed in a 50mL centrifuge bottles with 40 mL TAO solution. The solutions were shaken for 4 hours in the dark and the concentration of Al, Si, As, B, Cr and Se were measured by ICP-AES.

2.5 Desorption studies

In order to understand the association of oxyanions with allophane, phosphate extraction was carried out using 0.1M Na_2HPO_4 solution. Approximately 20 mg of each mineral samples was added to 40 mL of extractant solution and were shaken for 4 hours. The solid was separated by centrifugation and the supernatant was analysed for As, B, Cr and Se concentration using ICP-AES.

3. Results and discussiom

3.1 Characterization of precipitates

3.1.1 X-ray diffraction (XRD) analysis

The X-ray diffraction analysis confirmed that allophane was formed in the presence of As, B, Cr and Se. The profiles of all samples exhibited two broad peaks centered at 26.19^0 and 40.99^0 which are typical of natural allophane samples and amorphous aluminosilicates. Figure 3 and 4 show the XRD profiles of allophane samples with or without sorbed As and B, respectively (Cr and Se reacted allophane not shown since all samples have similar profile). One of these peaks especially the diffraction area between $25\text{-}27^0$ is specific to spherical hollow particles which originates from the SiO_4

tetrahedral sheet of allophane. The XRD profiles also show that the precipitates contain no crystalline impurities since the peaks that originate from aluminum hydroxides minerals such as boehmite and gibbsite were not observed but the diffraction peak of polymerized SiO_4 tetrahedral appears nearby at 22.78^0 [15]. Moreover, allophane precipitates with low Si/Al molar ratio showed prominent sharper peaks than with Si rich allophane.

3.1.2 FTIR spectroscopy of allophane samples

The IR spectra of synthetic allophane samples showed the typical characteristics of aluminosilicates minerals. For all samples with or without sorbed oxyanions, their IR spectra displayed a similar profile. Figure 5 presents the IR spectrum of pure allophane samples and with sorbed As and B, respectively (Cr and Se not shown). The corresponding peaks of individual elements were not detected since their concentration was very low relative to Al and Si which can overlap their corresponding vibration band. The intense vibration around 1000-900 cm^{-1} can be assigned to Si-O-(Si) or Si-O-(Al) vibration [16] and the shoulder at 870 cm^{-1} to Si-OH groups [17]. The vibration band in the region between 800-400 cm^{-1} can be attributed to aluminuous allophane subsheet of Al-O and Al-OH bonds [15, 16] and probably originated from the octahedral sheet

similar to the gibbsitic sheet present in imogolite structures [18, 19]. As the Si/Al ratio increases, the intensity of the bands around 680, 580 and 470 also increases. The difference between the spectra of Si and Al rich allophane is similar to the observations detected by Parfitt [18, 19] on natural allophane samples. The Si-rich allophane has an absorption maximum at 1020 cm^{-1} with relatively higher intensity compared to the Al-rich allophane at 975 cm^{-1}. Hence, the evolution of the spectra is influenced by the Si/Al ratio of allophane.

3.1.3 Surface charge characteristics

The surface charge characteristics as shown in Figure 6 presents the data of the potentiometric titration of pure synthesized allophane samples. The corresponding point of zero charge (PZC) for Al and Si rich allophane were 9.39 and 8.38 respectively. These PZC values were similar to synthesized amorphous aluminum hydroxide with PZC value of 9.1 in which the variable positive charge was also attributed to the surface aluminol groups [20]. It can be seen from the figure that the surface charge of the precipitates generate a variable positive charge at the acidic pH range up to the point of zero charge (PZC) value and a negative charge at the pH condition above the PZC value. Table 1 shows the PZC values of the mineral precipitates. The results also showed that

the PZC values of all precipitates were higher compared to natural allophane which lies at pH 5.5-6.5. The higher PZC values of synthesized allophane compared to natural allophane is due to the fact that the latter may already contain a considerable amount of adsorbed ions and organic matter in the soil solution [21]. It can also be seen from Table 1 that pure allophane samples with lower Si/Al ratio tend to have higher PZC values. The reason for this shift in the PZC value in relation to the Si/Al ratio is directly related to the change in the number of aluminol groups in the allophane surface which is the most reactive group compared to the silanol groups. The higher PZC value of allophane with lower Si/Al ratio is attributed to the larger concentration of aluminol groups which, under acidic or alkaline condition, become positively or negatively charged, respectively [22]. The influence of silanol groups on the surface charge characteristics of allophane was minimal since they are not placed on the external surface around the defect sites. Moreover, the weak influence of silica gel on the potentiometric studies may suggests that it does not contain OH groups [23]. If there is any, it will likely lower the measured zeta potential and PZC value of allophane samples since it has a variable negative charge at pH above 3.

3.2 Chemical analysis of precipitates

Table 1 gives the final Si/Al molar ratio of mineral precipitates after digestion with TAO solution and the remaining anion concentration. It is evident that there is no significant change with respect to the pure allophane samples in the final Si/Al molar ratio of the precipitates except for As(V) reacted allophane. The relatively lower final Si/Al ratio of allophane laden with As(V) can be directly related to the strong retention of As(V) compared to other anions. Moreover, the final Si/Al molar ratio of the precipitates also influenced the sorption behavior of As(V), Cr(VI), Se(VI) and boric acid onto allophane. Allophane samples with lower final Si/Al molar ratio tend to retain more oxyanions and boric acid than Si-rich allophane.

3.3 Sorption characteristics of oxyanions

The aqueous speciation of an element is one of the factors that determines the extent at which it is sorbed into the precipitating mineral phases. Under the experimental conditions used in this study, the speciation of the anions were determined by calculation using Act 2 code in Geochemist Workbench (GWB) [24]. Based on the calculation results, the dominant species exist as monomeric oxyanions (except for B) as $H_2AsO_4^-$, $B(OH)_3$, $HCrO_4^-$ and SeO_4^{2-}, respectively.

3.3.1 Adsorption studies

The order of preference for all four elements by allophane as shown in Table 1 is As >>> Se > B > Cr. Allophane exhibited very high removal efficiency for As(V) with more than 99% of arsenic were removed from the solution. However, allophane uptake for Cr(VI), Se(VI) and boric acid was low with only more than 30% removal efficiency for boric acid and Se(VI) and less than 20% for Cr(VI). The adsorption of these ionic species by allophane is expected since the synthesized allophane samples have a variable positive charge at circum-neutral pH condition as shown in Figure 6.

The large reduction of As(V) concentration after 24 hours of reaction time indicates that allophane has a strong affinity for As(V) and supports the fact that arsenic mobility in soils is limited by its capacity to be sorbed on soil components particularly by metal oxides, short-ranged ordered aluminosilicates [25] and Al and Fe hydroxides [26]. Evidently, Se(VI) adsorption was relatively higher, which is also consistent with well established results, that iron and aluminum oxide minerals are the most common geosorbents for selenium oxyanions [27]. However, the low uptake of boric acid and Cr(VI) by allophane suggests that ionic charge and anionic competition with silicate are the important factors that influence the extent of their retention, respectively. The corresponding low uptake of boric acid is largely due to its neutral charge

characteristics at circum-neutral pH condition. Thus, its electrostatic interaction with the reactive surface aluminol groups is at minimum compared to anionic species. On the other hand, competing anions have a drastic effect on Cr(VI) adsorption particularly when silicate anion is present [28]. The effect of silicate anion in inhibiting Cr(VI) adsorption can be supported by the presence of Si anions on allophane surfaces as observed by previous study of Arai [11]. Moreover, silicate anions can also be readily adsorbed by other variable charge minerals such as gibbsite and goethite [29, 30]. Since not all silicate anions reacted with aluminum during allophane synthesis, low chromate adsorption is expected.

The final Si/Al molar ratio of precipitates also influenced the adsorption characteristics of oxyanions and boric acid since the surface charge of allophane is strongly dependent on its Si/Al ratio. It can be seen from Table 1 that allophane with lower final Si/Al ratio tend to have higher removal efficiency. The higher removal efficiency of allophane with lower final Si/Al ratio was attributed to the increase in the amount of reactive surface aluminol groups which strongly influence the surface charge characteristics of allophane as revealed by potentiometric studies. This observation is in agreement with the lower removal efficiency of Si-rich allophane which showed lower variable positive charge density and PZC values. Moreover, the relatively low final

Si/Al ratio of allophane with adsorbed arsenate after adsorption experiments can be also attributed to the release of adsorbed Si in the allophane surface during As(V) adsorption [11].

3.3.2 Co-precipitation studies

The uptake behavior of oxyanions and boric acid during co-precipitation with allophane showed similar order of preference except that boric acid retention was slightly higher compared to Se(VI) in Al-rich allophane. The results also revealed that As(V) and boric acid uptake were relatively higher compared to adsorption experiments. Boric acid retention during co-precipitation with allophane of lower Si/Al ratio was substantially enhanced but not with Si-rich allophane. Similar results were also observed on As(V) sorption by aluminum oxides [25] and ettringite [31] in which higher retention of As(V) occured during co-precipitation experiments. These findings suggest that As(V) and boric acid incorporation into the allophane structure is one of the dominant mechanisms in addition to surface adsorption. Moreover, Se(VI) uptake during co-precpitation with allophane showed contrasting behavior between Al and Si rich allophane. Only high Al content allophane showed significant increase in Se(VI) retention during co-precipitation, which may also suggest its incorporation in the

allophane structure. The reason for the decrease in Se (VI) uptake by Si rich allophane during co-precipitation compared to adsorption experiments is unclear to the authors and further investigation is required to confirm this behavior. Chromate retention on the other hand, showed no significant difference compared to adsorption experiments which indicates that its retention by allophane are mainly controlled by surface adsorption. On the other hand, the final Si/Al molar ratio of allophane also influenced the uptake behavior of oxyanions and boric acid in which Al-rich allophane showed higher retention capacity.

3.4 Desorption of oxyanions

The desorption efficiency of oxyanions and boric acid after leaching experiments using phosphate as desorbing ligand is shown in Figure 7. The figure clearly shows that large amount of adsorbed oxyanions and boric acid were easily replaced by phosphate. This result indicates that the presence of competing anions with strong affinity to allophane such as phosphate can easily release the adsorbed oxyanions from the allophane surface. Allophane is known to fix phosphate strongly than any other anions [32]. In contrast, only co-precipitated As(V) and boric acid showed significant reduction of leached amount after desorption experiments. This results agree with the

previous findings described earlier that incorporation and surface adsorption governed As(V) and boric acid retention while only surface adsorption for Cr(VI) and Se(VI) during co-precipitation experiments. Similar results were also observed by Violante [25] in which less amount of As(V) was released due to phosphate adsorption onto Al and Fe oxides minerals with co-precipitated arsenate. In the case of Se(VI), even though it showed enhanced retention by Al rich allophane during coprecipitation, the fact that it was easily release during desorption experiments suggests that its retention by allophane is mainly controlled by surface adsorption. Moreover, the desorption of As(V) was also influenced by the Al content of allophane in which lesser amount of As(V) was leached from Al rich allophane (Figure 7a).

3.5 Sorption mechanisms of oxyanions and boric acid by allophane

3.5.1 Adsorption studies

The zeta potential is the potential at the shear or slipping plane which exists at the interface of a mineral and the surrounding liquid [33]. This slipping plane is placed slightly outside of the d-plane which is a border with a diffusion layer in the Triple-Layer model by Hayes [34]. The formation of complexes inside the slipping plane strongly affects the zeta potential. Since inner-complexes are formed inside the

shear plane, significant changes in the zeta potential can be expected. The substantial decrease in the zeta potential attributed to the inner-sphare, bidentate surface complex of HPO_4^{2-} on the hydrotalcite surface was already observed by Lagaly [35]. On the other hand, outer-sphere complexes are distributed over the diffuse layer outside the slipping plane and thus, do not affect the zeta potential. However, outer-sphere complexes with strong electrostatic interaction that form in the slipping plane may also affect the zeta potential as in the case of SO_4^{2-}, CO_3^{2-} and CrO_4^{2-} [36].

The significant shift of the PZC value to lower pH and the decrease of zeta potential after adsorption of As(V) and boric acid as shown in Figure 8a and 8b may also indicate that the binding of these ions on allophane surface with the surface aluminol group is governed by inner-sphere complexation through oxygen sharing. The presence of inner-sphere bidentate binuclear surface species on aluminum octahedral structures during As(V) adsorption by allophane was already confirmed by XAS analysis [11]. The findings of Su and Suarez [17] and Son [14] also concluded that boric acid sorption on allophane is via inner-sphere complexation. In contrast, the surface charge characteristics of allophane after Cr(VI) and Se(VI) adsorption showed no significant change which indicates that the binding is largely controlled by outer-sphere complexation (Figure 7c and 7d). Using EXAFS spectroscopy, Peak [27] concluded that

Se(VI) adsorption on the surface of hydrous aluminum oxide primarily forms outer-sphere complexes. On the other hand, the adsorption of oxyanions and boric acid on polymerized silica is not supported because it did not contain OH groups as revealed by zeta potential measurement. If there is any, the electrostatic interaction of silica gel with the oxyanions and boric acid is unlikely as they have both negative charges (except for B) at near neutral pH condition. Moreover, the binding strength of any anions on the adsorption sites depends on their specific ionic properties such as ionic charge (z) and radius (r). In general, the higher the ionic potential (Ip = z/r), the more covalent its bonding and more inner-sphere the complex [37].

3.5.2 Co-precipitation studies

Based on the phosphate extraction experiments, surface adsorption and incorporation into the allophane structure are the two possible mechanisms of As(V) and boric acid uptake during co-precipitation with allophane while the former largely controls Cr(VI) and Se(VI) uptakes. The sorption of As(V) and boric acid duirng co-precipitation also showed significant reduction of zeta potential (data not shown) and PZC value of allophane but not with Cr(VI) and Se(VI).

The incorporation of As(V) into the allophane structure during co-precipitation with allophane may occur via direct substitution of Si in the inner tetrahedral layer. The occurrence of As(V) in the tetrahedral site of silicate minerals was already detected in minerals such as antigorite [38] and andraditic garnet [39]. The similarity of atomic properties such as ionic radius and coordination number of As(V) and Si anion may account for the strong incorporation of As(V) during allophane formation. On the other hand, detailed study of Henmi [40] concluded that allophane with higher Si/Al ratio of more than 0.5 has excess Si atom weakly attached to the SiO_4 tetrahedra around the defect sites of allophane as shown in Figure 9. Hence, structural substitution for this weakly attached Si may also account for As(V) and boric acid incorporation in the allophane structure. The difference in coordination number of trigonally coordinated boric acid and Si tetrahedral may strongly inhibit the direct substituion of Si by boric acid in the tetrahedral site.

On the other hand, the inability of Cr(VI) and Se(VI) oxyanions to replace Si during co-precipitation with allophane may probably result to charge imbalance in the tetrahedral site [38,39]. Although As(V) and Se(VI) have similar size and the same tetrahedral structure, strict structural considerations cannot account for the different

behavior of oxyanions and do not provide a satisfactory explanation for anion site preferences [1].

4. Conclusions

As confirmed by the leaching test using phosphate bearing solution, this sudy showed that As(V) and boric acid can be irreversibly fixed during co-precipitation with allophane. However, Cr(VI) and Se(VI) retention during and after allophane precipitation is mainly controlled by surface adsorption. The structurally fixed As(V) is presumed to be incorporated within the allophane structure, replacing Si in the inner tetrahedral layer and the weakly attached Si in the defect sites. The latter may governed boric acid incorporation. The incorporated As(V) and boric acid were more resistant to release than those bound on the mineral surface. On the other hand, the retention of As(V) and boric acid on the allophane surface mainly involved inner-sphere complexation while Cr(VI) and Se(VI) sorption is governed by outer-sphere complexation. Allophane also showed high selectivity for As(V) compared to other oxyanions and boric acid. The sorption characteristics of oxyanions and boric acid was also influenced by the final Si/Al molar ratio of allophane in which Al-rich allophane tend to have higher uptake capacity.

The overall results of this study have demostrated the role of allophane-like nanoparticles and the effect of its Si/Al ratio on As, B, Cr and Se transport processes in the subsurface environment. The uptake mechanisms of allophane for various anions may also suggest a similar process on amorphous aluminosilicate on aquifer, soils and other soil minerals. This study also provides insight on the possibility of using allophane nanoparticles for water treatment and soil remediation.

Acknowledgements

The authors would like to thank Kazuya Morimoto and Atsushi Asai (Hokkaido University) for their assistance in doing the ICP-AES and Zeta Potential measurements. Thanks are also due to Remel Salamingo (Hokkaido University) for extending his skills using SolidWorks software in redrawing the proposed atomic structure of nano-ball allophane. Lastly, the authors would like to thank the two anonymous reviewers for their thoughtful suggestions and comments which greatly improved the manuscript.

References

[1] V.G. Alexandratos, E.J. Elzinga, R.J. Reeder, Arsenate uptake by calcite: Macroscopic and spectroscopic characterization of adsorption and incorporation mechanisms. Geochimica et Cosmochimica Acta. 71 (2007) 4172-4187.

[2] N. Sahai, Y.J. Lee, H. Xu, M. Ciardelli, J. Gaillard, Role of Fe(II) and phosphate in arsenic uptake by co-precipitation. Geochimica et Cosmochimica Acta. 71 (2007) 3193-3210.

[3] O.P. Ferreira, S.G. de Moraes, N. Duran, L. Cornejo, O.L. Alves, Evaluation of boron removal from water by hydrotalcite-like compounds. Chemosphere 62 (2006) 80-88.

[4] Y. Tang, E.J. Elziga, Y.J. Lee, R.J. Reeder, Co-precipitation of chromate with calcite: Batch experiments and X-ray absorption spectroscopy. Geochimica et Cosmochimica Acta. 71 (2007) 1480-1493.

[5] M. Zhang, E.J. Reardon, Removal of B, Cr, Mo and Se from wastewater by incorporation into hydrocalumite and ettringite. Environmental Science and Technology. 37 (2003) 2947-2952.

[6] B.K.G Theng, G. Yuan, Nanoparticles in the soil environment. Elements. 4 (2008) 395-399.

[7] T. Henmi, K. Wada, Morphology and composition of allophane. American Mineralogist. 61 (1976) 379-390.

[8] Z. Abidin, N. Matsue, T. Henmi, Differential formation of allophane and imogolite: experimental and molecular orbital study. Journal of Computer-Aided Materials and Design. 14 (2007) 5-18.

[9] B.K.G. Theng, M. Rusell, G.J. Churchman, R.L. Parfitt, Surface properties of allophane, halloysite and imogolite. Clays and Clay Minerals. 30(2) (1982) 143-149.

[10] C. Zevenbergen, J.P. Bradley, L.P. Van Reeuwijk, A.K. Shyam, O. Hjelmay, R.N. Comans, Clay formation and metal fixation during weathering of coal fly ash. Environmental Science and Technology. 33 (1999) 3405-3409.

[11] Y. Arai, D.L. Sparks, J.A. Davis, Arsenate adsorption mechanisms at the Allophane-water interface. Environmental Science and Technology. 39 (2005) 2537-2544.

[12] G. N. Padilla, N. Matsue, T. Henmi, Change in charge properties of nano-allophane as influenced by sulfate adsorption. Clay Science. 12 (2002) 33-39.

[13] E.A. Elhadi, N. Matsue, T. Henmi, Adsorption of molybdate on nan-ball allophane. Clay Science. 11 (2000) 189-204.

[14] L.T. Son, N. Matsue, T. Henmi, Boron adsorption on allophane with nano-ball morphology. Clay Science. 10 (4) (1998) 315-325.

[15] F. Ohashi, S.I. Wada, M. Suzuki, M. Maeda, S. Tomura, Synthetic allophane from high concentration solutions: nanoengineering of the porous solid. Clay Minerals. 37 (2002) 451-456.

[16] E. Montarges-Pelletier, S. Bogenez, M. Pelletier, A.Razafitianamaharavo, J. Ghanbaja, B. Lartiges, L. Michot, Synthetic allophane-like particles: textural properties. Colloids and Surfaces A: Physicochemical Engineering Aspects. 255 (2005) 1-10.

[17] C. Su, D.L. Suarez, Boron sorption and release by allophane. Soil Science Society of America Journal. 61 (1) (1997) 69-77.

[18] R.L. Parfitt, R.J. Furkert, T. Henmi, Identification and structure of two types of allophane from volcanic ash soils and tephra. Clays and Clay Minerals. 28 (5) (1980) 328-334.

[19] R.L. Parfitt, T. Henmi, Structure of some allophanes from New Zealand. Clays and Clay Minerals. 28 (4) (1980) 285-294.

[20] K. Fukushi, K. Tsukimura, H. Yamada, Surface acidity of amorphous aluminum hydroxide. Acta Geologica Sinica. 80(2) (2006) 206-211.

[21] E. Hanudin, N. Matsue, T. Henmi, Change in charge characteristics of allophane with adsorption of low molecular weight organic acids. Clay Science. 11 (2000) 243-255.

[22] R. L. Parfitt, Allophane in New Zealand – A review. Australian Journal of Soil Research. 28 (1990) 343-360.

[23] L. Denaix, I. Lamy, J.Y. Bottero, Structure and affinity towards Cd2+, Cu2+, Pb2+ of synthetic colloidal amorphous aluminosilicates and their precursors. Colloids and Surfaces A: Physicochemical Engineering Aspects. 158 (1999) 315-325.

[24] C.M. Bethke, Geochemical reaction modelling: concepts and applications. Oxford University Press, New York, New York, 1996.

[25] A. Violante, M. Ricciardella, S. Del Gaudio, M. Pigna, Co-precipitation of arsenate with metal oxides: Nature, mineralogy, and reactivity of aluminum precipitates. Environmental Science and Technology. 40 (2006) 4961-4967.

[26] Y. Masue, R.H. Loeppert, T.A. Kramer, Arsenate and arsenite adsorption and desorption behavior on co-precipitated aluminum:iron hydroxides. Environmental Science and Technology. 41 (2007) 837-842.

[27] D. Peak, Adsorption mechanisms of selenium oxyanions at the aluminum oxide/water interface. Journal of Colloids and Interface Science. 303 (2006) 337–345.

[28] F.C. Richard, A.C. Bourg, Aqueous geochemistry of chromium: A review. Water Research. 25 (7) (1991) 807-816.

[29] F. J. Hingston, A.M. Posner, J.P. Quirk, Anion adsorption by goethite and gibbsite. 1. The role of the proton in determining adsorption envelop. Journal of Soil Science. 23 (1972) 177-195.

[30] L. Sigg, W. Stumm, The interaction of anions and weak acids with hydrous goethite surface. Colloids Surfaces. 2 (1981) 101-117.

[31] S. Myneni, S.J. Traina, T.J. Logan, G.A. Waychunas, Oxyanions behavior in alkaline environments: Sorption and desorption of arsenate in ettringite. Environmental Science and Technology. 31 (1997) 1761-1768.

[32] R. L. Parfitt, Phosphate reactions with natural allophane, ferrihydrite and goethite. Journal of Soil Science. 1989, 40, 359-369.

[33] R.J. Hunter, Zeta Potential in Colloid Science. Academic Press, London, 1981.

[34] K.F. Hayes, G. Redden, W. Ela, J.O. Leckie, Surface complexation models: An evaluation model parameter-estimation using FITEQL and oxide mineral titration data. Journal of Colloid and Interface Science. 142(2) (1991) 448-469.

[35] G. Lagaly, O. Mecking, D. Penner, Colloidal magnesium aluminum hydroxide and heterocoagulation with a clay mineral. I. Properties of colloidal magnesium aluminum hydroxide. Colloid and Polymer Science. 279(11) (2001) 1090-1096.

[36] L. Chatelet, J.Y. Bottero, J. Yvon, A. Bouchelaghem, Competition between monovalent and divalent anions for clacined and unclacined hydrotalcite: Anion exchange and adsorption sites. Colloids and Surfaces A: Physico-chemical and Engineering Aspects. 111(3) (1996) 167-175.

[37] D. Langmuir, Aqueous environmental geochemistry. Prentice Hall Inc., Upper Saddle River, New Jersey, 1997.

[38] K. Hattori, Y. Takahashi, S. Guillot, B. Johanson. Occurrence of arsenic (V) in forearc mantle serpentinites based on X-ray absorption spectroscopy study. Geochimica et Cosmochimica Acta. 69(23) (2005) 5585-5596.

[39] J.M. Charnock, D.A. Polya, A.G. Gault, R.A. Wogelius, Direct EXAFS evidence for incorporation of As^{5+} in the tetrahedral site of natural andraditic garnet. American Mineralogist. 92 (2007) 1856-1861.

[40] T. Henmi, N. Matsue, E. Johan, Change in the surface acidity of allophane with low Si/Al ratio by reaction with orthosilicic acid. Japan Journal of Soil Science and Plant Nutrition. 68 (1997) 514-520 (in Japanese with english abstract).

Figure Captions

Figure 1. Structural model of allophane. Reproduced after [12].

Figure 2. TEM image of pure allophane with initial Si/Al = 0.67.

Figure 3. XRD profiles of arsenate reacted allophanes.(A) As sorption with initial Si/Al ratio = 0.67. (B) As sorption with initial Si/Al ratio = 1.0.

Note: (a) without sorbed anions, (b) after adsorption, (c) after co-precipitation.

Figure 4. XRD profiles of boric acid reacted allophanes. (A) B sorption with initial Si/Al ratio = 0.67. (B) B sorption with initial Si/Al ratio = 1.0.

Note: (a) without sorbed anions, (b) after adsorption, (c) after co-precipitation.

Figure 5. FTIR spectra of allophane precipitates. (A) allophane with initial Si/Al ratio of 0.67 reacted with arsenate. (B) allophane with initial Si/Al ratio of 1.0 reacted with B.

Note: (a) allophane without sorbed anions; (b) after adsorption (c) after co-precipitation.

Figure 6. Surface charge characteristics of allophane without sorbed anions.

Figure 7. Desorption efficiency of oxyanions after phosphate extraction. (a) allophane with lower final Si/Al ratio. (b) allophane with higher final Si/Al ratio.

Figure 8. Surface charge characteristics of allophane samples after adsorption. (a and c) allophane with initial Si/Al ratio = 0.67. (b and d) allophane with initial Si/Al ratio = 1.0

Figure 9. Structure of nano-ball allophane around the defect sites. Redrawn from [12].

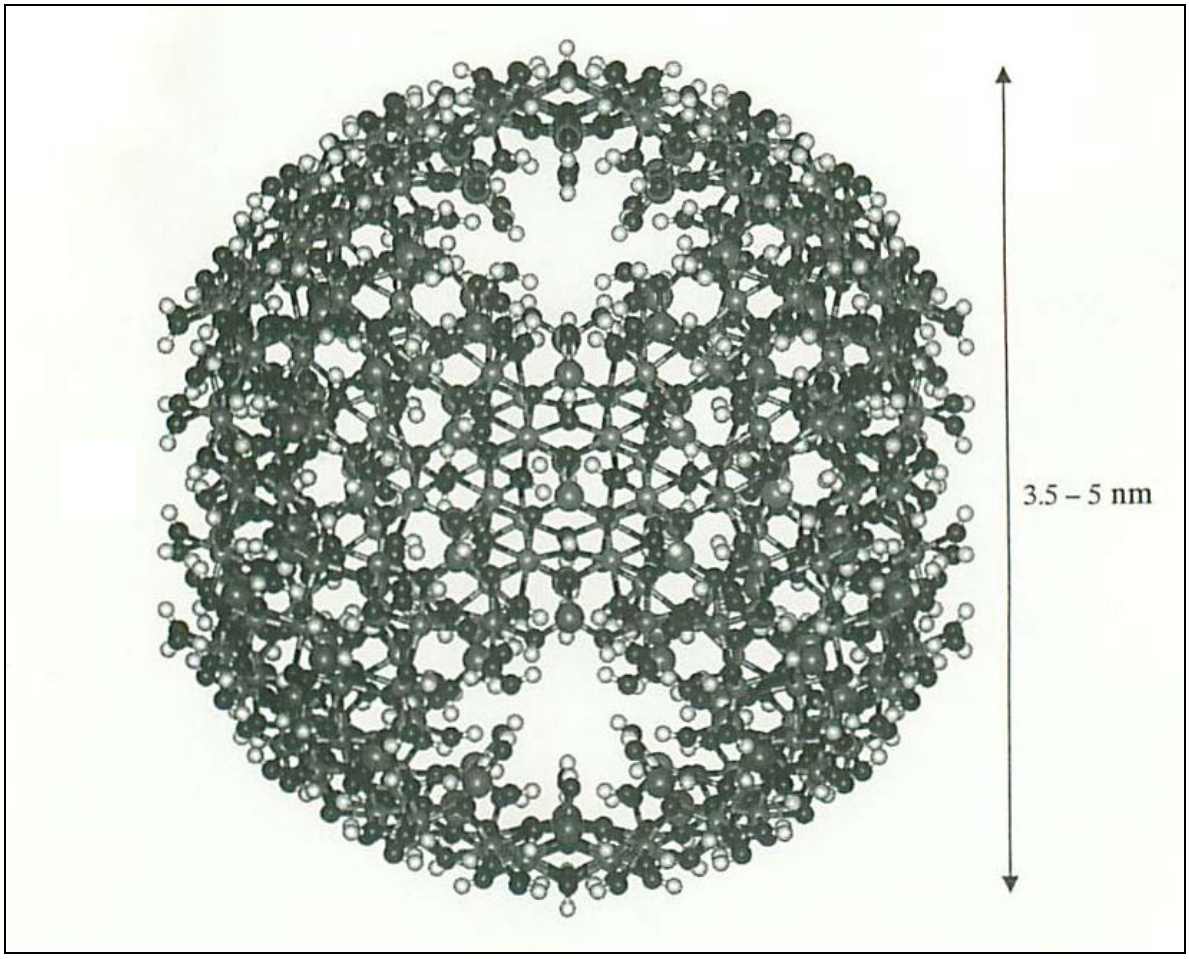


Figure 1

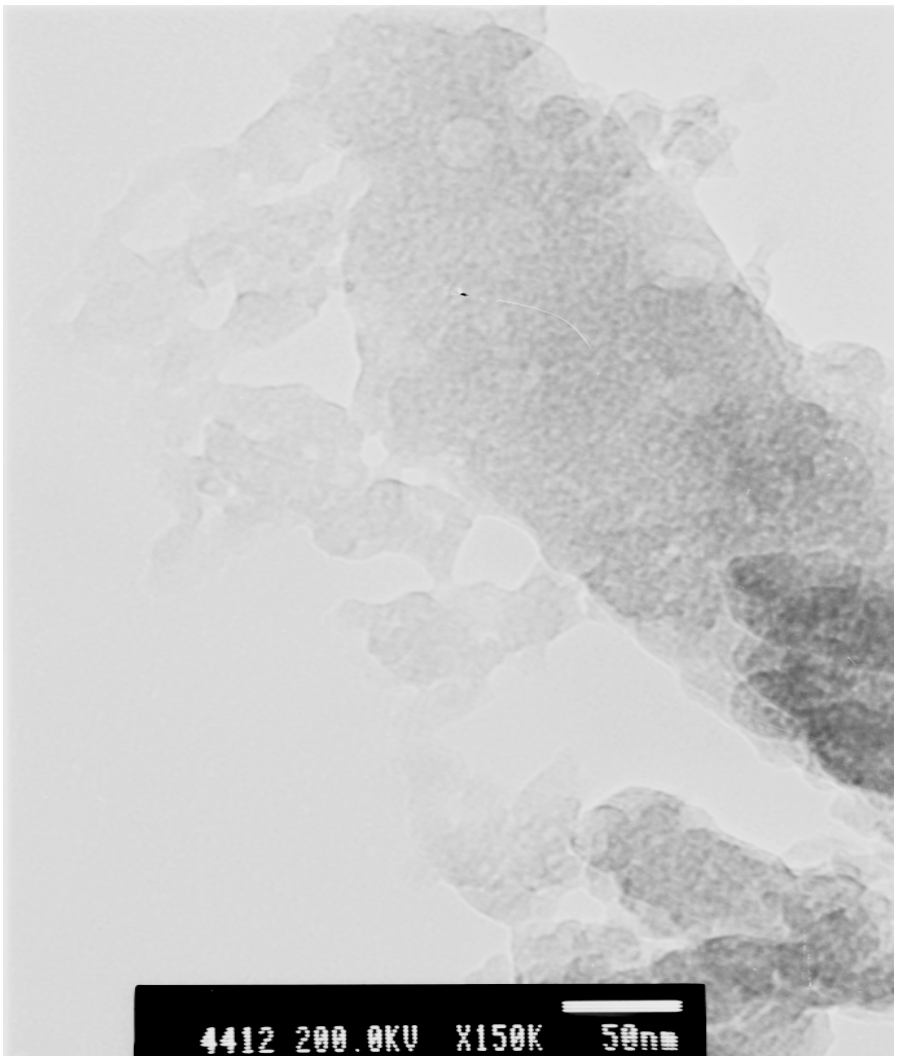


Figure 2

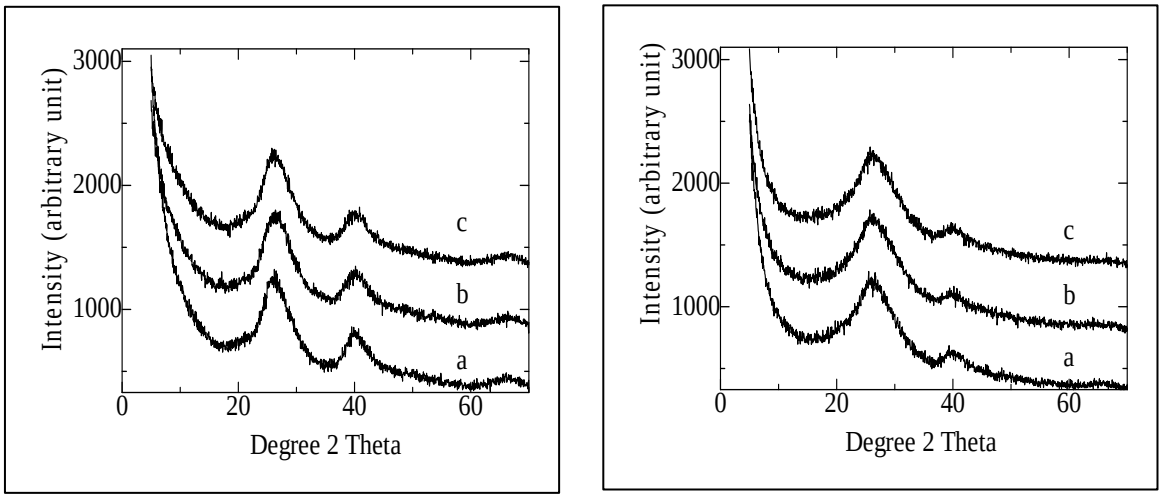


Figure 3

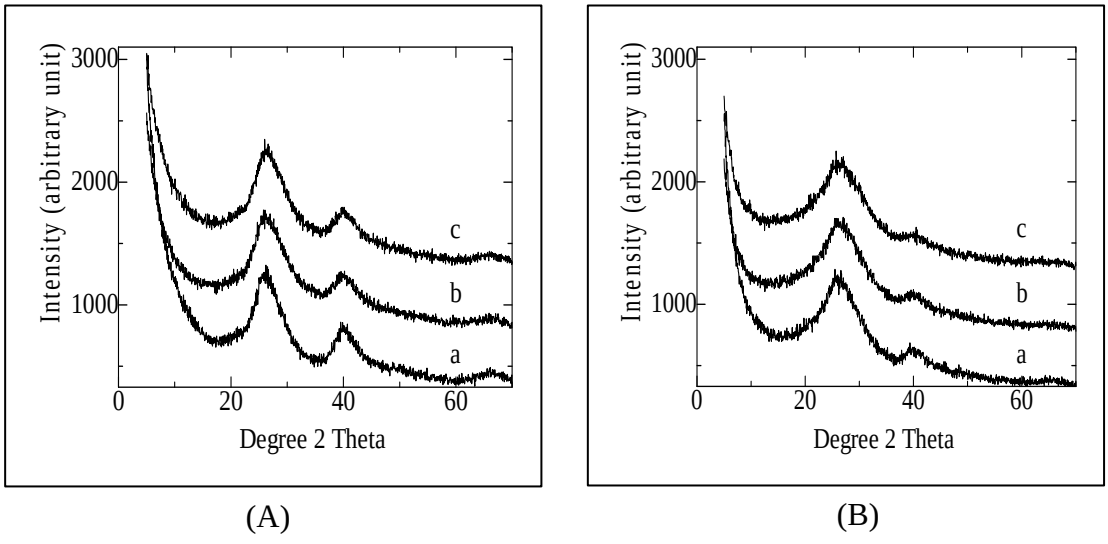
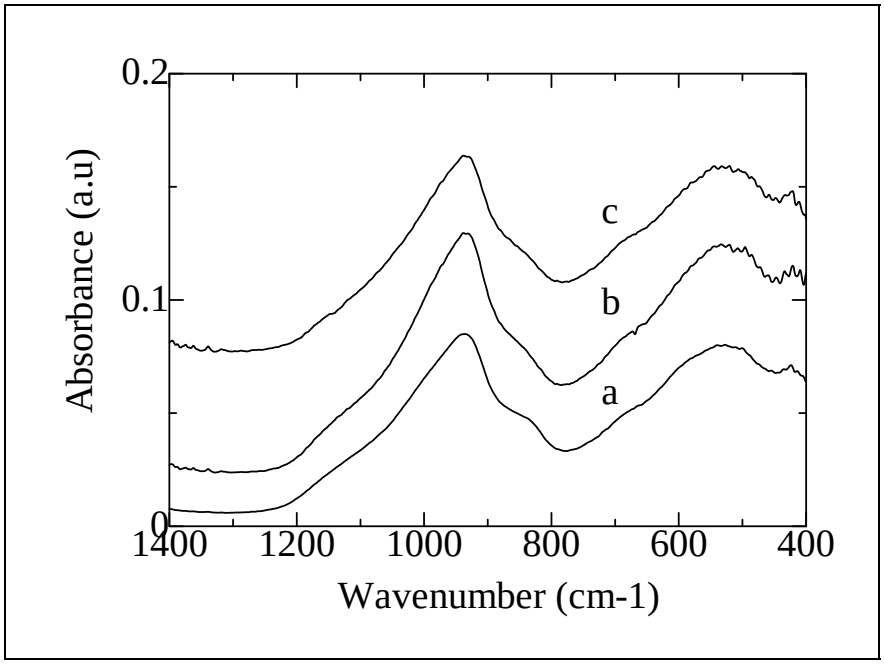
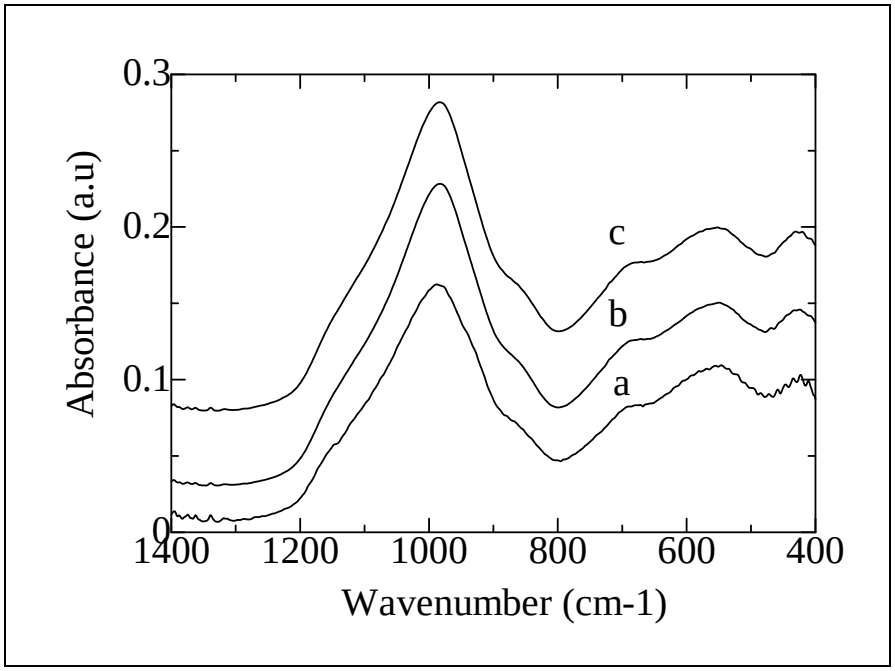


Figure 4


0.2
0.1
0
Absorbance (a.u)
c
b
a
1400
1200
1000
800
600
400
Wavenumber (cm-1)

(A)


0.3
0.2
0.1
0
Absorbance (a.u)
c
b
a
1400
1200
1000
800
600
400
Wavenumber (cm-1)

(B)

Figure 5

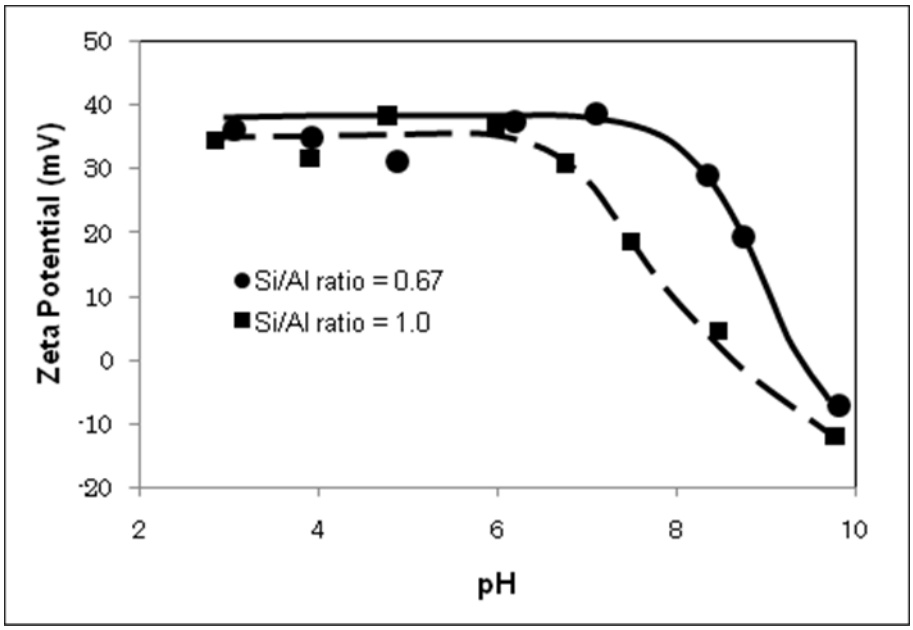
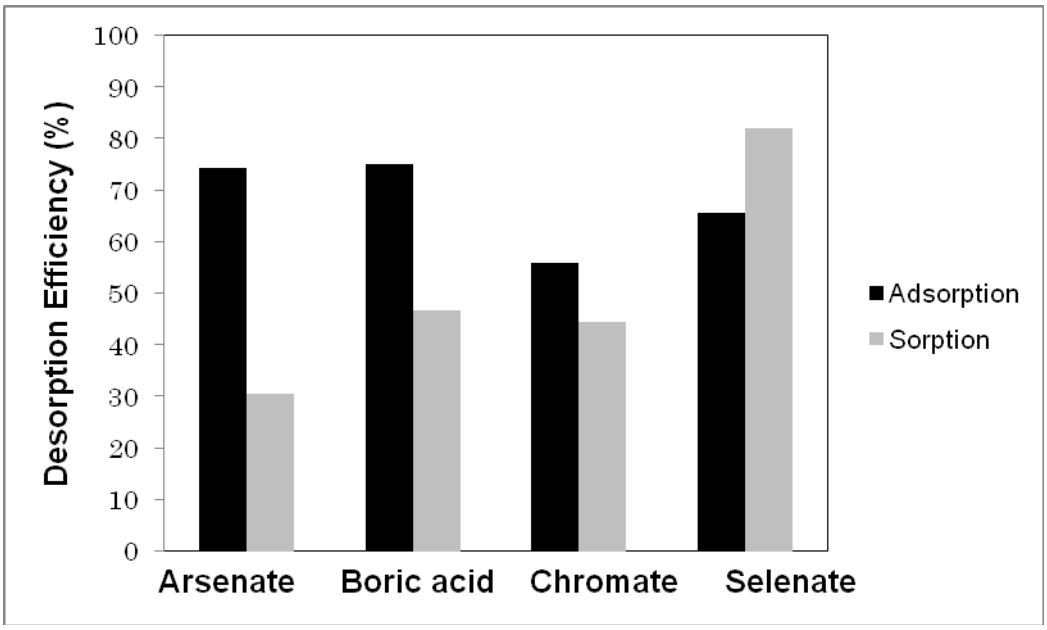
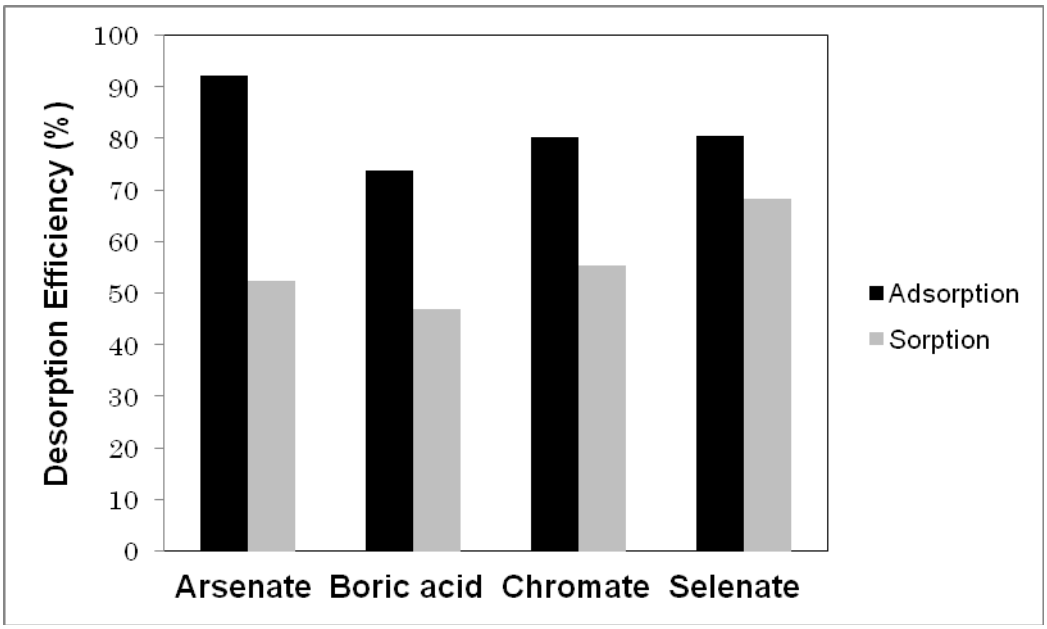

Zeta Potential (mV)
50
40
30
20
10
0
-10
-20
2
4
6
8
10
pH
Si/Al ratio = 0.67
Si/Al ratio = 1.0

Figure 6

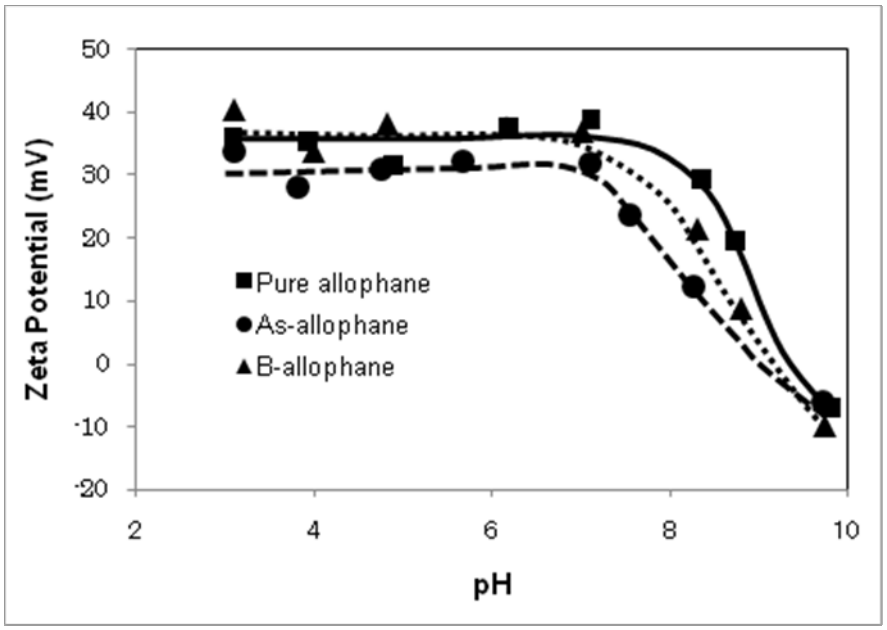

Desorption Efficiency (%)
100
90
80
70
60
50
40
30
20
10
0
Arsenate
Boric acid
Chromate
Selenate
Adsorption
Sorption

(a)

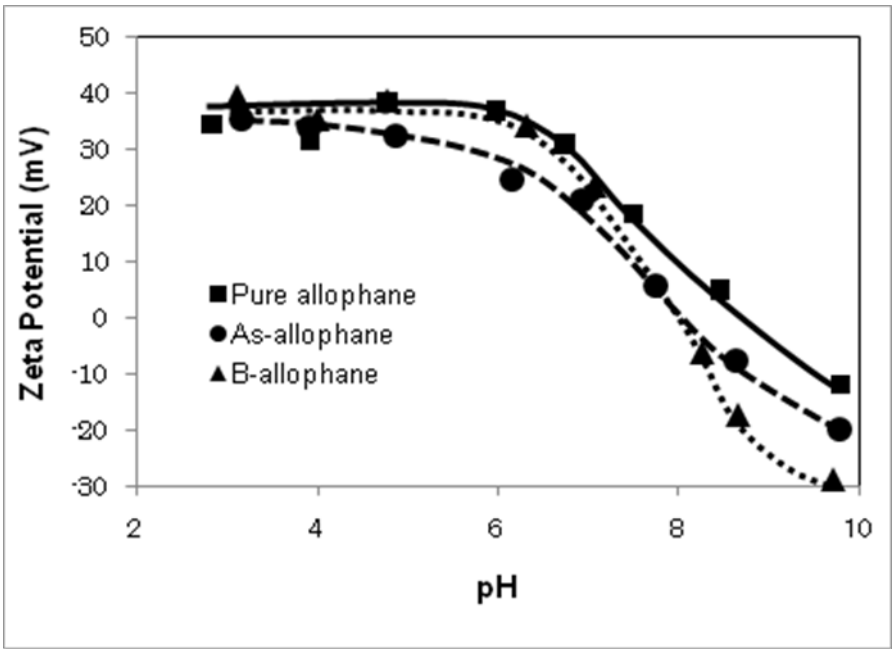

Desorption Efficiency (%)
100
90
80
70
60
50
40
30
20
10
0
Arsenate
Boric acid
Chromate
Selenate
Adsorption
Sorption

(b)

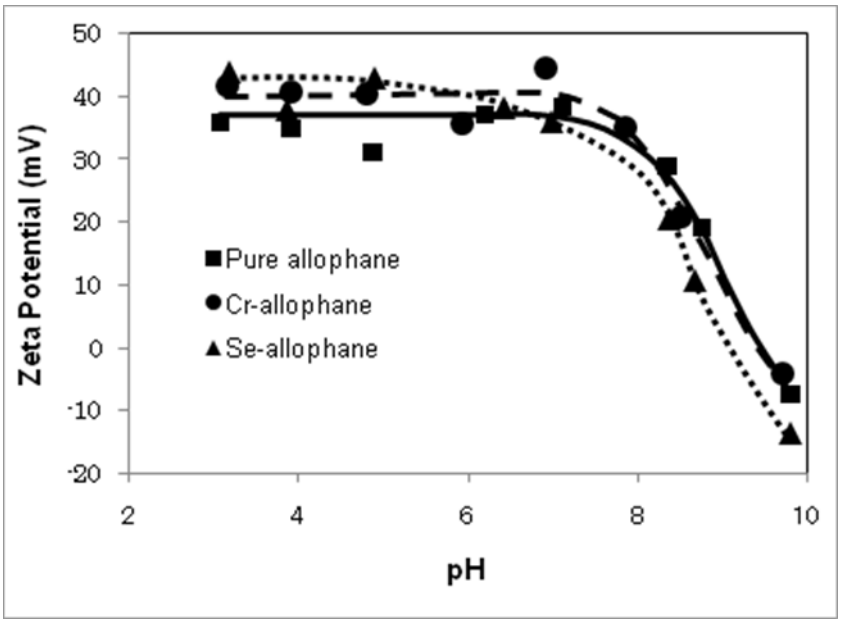
Figure 7


Zeta Potential (mV)
50
40
30
20
10
0
-10
-20
2
4
6
8
10
pH
Pure allophane
As-allophane
B-allophane

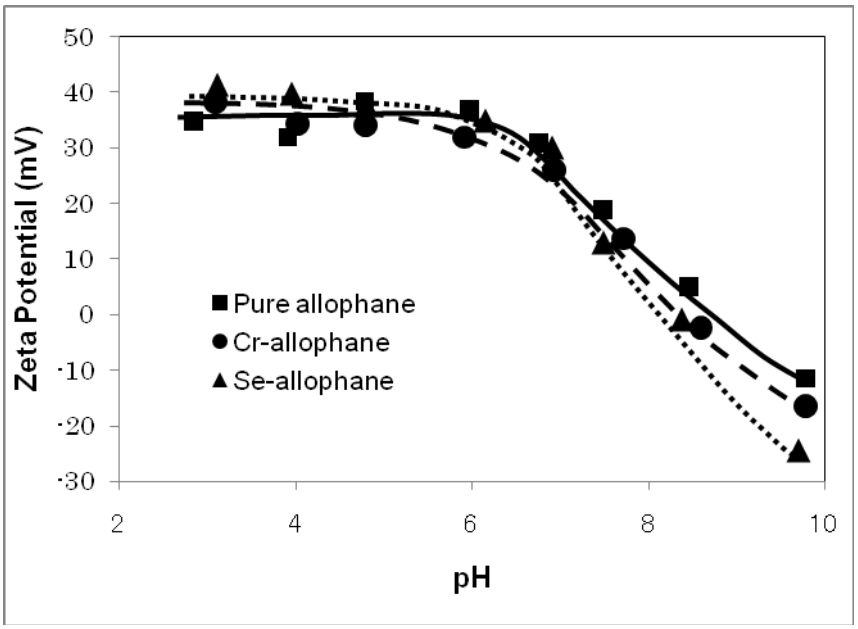
(a)


Zeta Potential (mV)
50
40
30
20
10
0
-10
-20
-30
2
4
6
8
10
pH
Pure allophane
As-allophane
B-allophane

(b)


Zeta Potential (mV)
50
40
30
20
10
0
-10
-20
2
4
6
8
10
pH
Pure allophane
Cr-allophane
Se-allophane

(c)


Zeta Potential (mV)
50
40
30
20
10
0
-10
-20
-30
2
4
6
8
10
pH
Pure allophane
Cr-allophane
Se-allophane

(d)

Figure 8

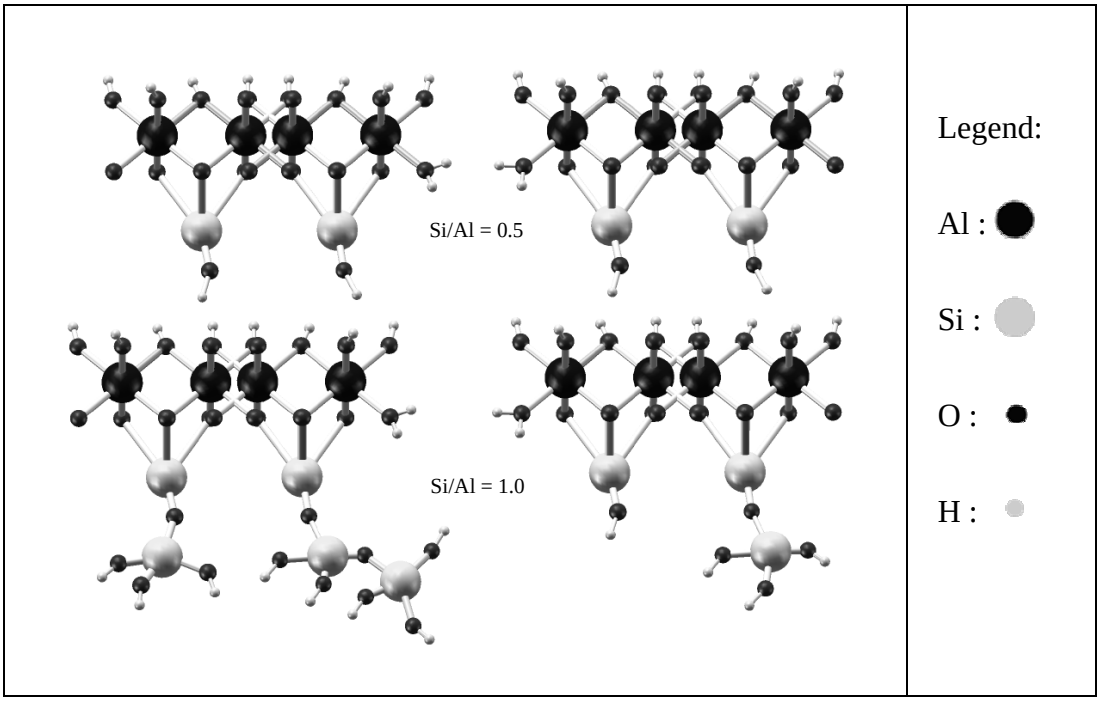


Figure 9

Table 1. Results of oxyanion sorption by allophane, final Si/Al molar ratio and PZC values of allophane precipitates.

Sample	Sorbed oxyanion	Final Si/Al ratio	PZC value	Residual anion concentration (mg/L)
All-067	N/A	0.52	9.39	N/A
All-100		0.78	8.38	N/A
All-S067	As	0.46	9.05	0.03
All-S100		0.50	8.04	0.33
All-C067		0.43	9.22	< 0.01
All-C100		0.37	8.16	< 0.01
All-S067	B	0.57	9.14	6.46
All-S100		0.81	7.82	8.67
All-C067		0.54	8.91	4.75
All-C100		0.81	7.93	8.04
All-S067	Cr	0.53	9.43	7.57
All-S100		0.79	8.32	9.32
All-C067		0.52	9.42	7.64
All-C100		0.79	8.40	9.05
All-S067	Se	0.55	9.13	6.17
All-S100		0.81	8.15	4.68
All-C067		0.57	9.39	4.91
All-C100		0.81	8.13	6.69

Note: All-S067: adsorption with intial Si/Al = 0.67; All-S100: adsorption with intial Si/Al = 1.0; All-C067: coprecipitation with initial Si/Al = 0.67 and All-C100: coprecipitation with initial Si/Al = 1.0, N/A = Not applicable